REPORT DOCUMENTATION PAGE

Form Approved
OMB NO. 0704-0188

1. AGENCY USE ONLY (Leave Blank)	2. REPORT DATE	3. REPORT TYPE AND DATES COVERED
	07.02.07	Final Progress Report 10.01.06 - 06.30.07

4. TITLE AND SUBTITLE

Losses and Degradation in Nanoscale Frequency Control Resonator

5. FUNDING NUMBERS

W911NF-06-1-0491

6. AUTHOR(S)

Prof. G. J. Iafrate and Prof. A. A. Kiselev

7. PERFORMING ORGANIZATION NAME(S) AND ADDRESS(ES)

North Carolina State University Research Administration & Sponsored Program Services 2 Leazer Hall Room 1 2230 Stinson Dr. Raleigh, NC, 27695-7514

8. PERFORMING ORGANIZATION REPORT NUMBER

9. SPONSORING / MONITORING AGENCY NAME(S) AND ADDRESS(ES)

U. S. Army Research Office
P.O. Box 12211
Research Triangle Park, NC 27709-2211

10. SPONSORING / MONITORING AGENCY REPORT NUMBER

51961.1-EG-II

11. SUPPLEMENTARY NOTES

The views, opinions and/or findings contained in this report are those of the author(s) and should not be construed as an official Department of the Army position, policy or decision, unless so designated by other documentation.

12 a. DISTRIBUTION / AVAILABILITY STATEMENT

Approved for public release; distribution unlimited.

12 b. DISTRIBUTION CODE

13. ABSTRACT (Maximum 200 words)

The objective is to identify loss and degradation mechanisms relevant to the frequency control resonator performance as the resonator dimensions reduce to the nanodimensional spatial scale. The Department of Army interest in scaling such devices into the nanodimensional region stems from the technical projection that such resonators can operate at frequencies into the low GHz spectral region thus providing a low cost, integratable NEMS solid state device option for frequency control electronic applications relevant to secure communications. The key questions regarding NEMS resonator performance are the fundamental physical limitations that arise in quality factor Q and noise figure as the resonator is reduced to nanodimensions in order to achieve the higher frequencies of device operation. Such physical limitations may also present barriers in other NEMS smart actuator and sensor electronic device applications. The technical approach considers non-equilibrium heat generation and redistribution processes from mechanical strain during high frequency NEMS operation beyond the conventional heat diffusion and local temperature approximation. A semiclassical phonon dynamical picture is introduced to go beyond the conventional models. Scaling laws relevant to the appropriate phonon transport regimes and their transition boundaries are delineated, analyzed, and compared with results of detailed microscopic descriptions. Thus, the research approach involves scaling analysis, coupled with analytical and numerical modeling of phonon flow and heat redistribution in nanoscale resonators.

14. SUBJECT TERMS

15. NUMBER OF PAGES
20

16. PRICE CODE

17. SECURITY CLASSIFICATION OR REPORT	18. SECURITY CLASSIFICATION ON THIS PAGE	19. SECURITY CLASSIFICATION OF ABSTRACT	20. LIMITATION OF ABSTRACT
UNCLASSIFIED	**UNCLASSIFIED**	**UNCLASSIFIED**	**UL**

NSN 7540-01-280-5500

Standard Form 298 (Rev.2-89)
Prescribed by ANSI Std. 239-18
298-102

Losses and Degradation in Nanoscale Frequency Control Resonator

G. J. Iafrate and A. A. Kiselev
North Carolina State University, Raleigh, NC 27695

Contents

1 Report Summary **2**

2 Approach, rationale, and accomplishments **5**
2.1 Picture of the beam dynamics. 5
2.1.1 Structure of the strain field 7
2.1.2 Mode energy density and total mechanical energy 8
2.2 Intrinsic dissipation mechanisms and their scaling 8
2.2.1 Fourier's law 9
2.2.2 Akhiezer effect 10
2.2.3 Scaling of losses with resonator dimensions 11
2.3 Phonons under non-equilibrium thermodynamic conditions in flexural nanobeams . 11
2.3.1 Phonon Hamiltonian in presence of strain 12
2.3.2 Boltzmann equation 13
2.3.3 Phonon related losses in flexural beams 15
2.3.4 Analysis of internal thermal phonon flow inside the beam in the (comparatively simple) limit of large aspect ratio $L/t \gg 1$ ($L \approx$ ultrasubmicron) . 16
2.4 Surface effects 17
2.4.1 Boundary conditions at beam interfaces for phonon distribution function . 18
2.5 Final observations 18

References **20**

1 Report Summary

Objective:

The objective is to identify loss and degradation mechanisms relevant to the frequency control resonator performance as the resonator dimensions reduce to the nanodimensional spatial scale. The Department of the Army interest in scaling such devices into the nanodimensional region stems from the technical projection that such resonators can operate at frequencies into the low GHz spectral region thus providing a low cost, integratable NEMS solid state device option for frequency control electronic applications relevant to jam resistant secure communications. The key questions regarding NEMS resonator performance are the fundamental physical limitations that arise in quality factor Q and noise figure as the resonator is reduced to nanodimensions in order to achieve the higher frequencies of device operation. Such physical limitations may also present barriers in other NEMS smart actuator and sensor electronic device applications.

Approach:

The technical approach considers non-equilibrium heat generation and redistribution processes from mechanical strain during high frequency NEMS operation beyond the conventional heat diffusion and local temperature approximation. A semiclassical phonon dynamical picture is introduced to go beyond the conventional models. Scaling laws relevant to the appropriate phonon transport regimes and their transition boundaries are delineated, analyzed, and compared with results of detailed microscopic descriptions. Thus, the research approach involves scaling analysis, coupled with analytical and numerical modeling of phonon flow and heat redistribution in nanoscale resonators. Specifically, the following technical milestones were pursued:

1. Establish a picture of the beam dynamics in a non-equilibrium thermodynamical framework. This requires a more refined look at the approximations of the Euler-Bernoulli equation both with and without the Timoshenko rotational inertia and shear corrections to the beam dynamics, and generalizations of stress-strain relations in the presence of thermal gradients.

2. For intrinsic phonon-mediated dissipation mechanisms, formulate scaling laws based on relations between the key spatial and temporal characteristics of phonons, i.e., mean free path l_{ph} and phonon relaxation time τ_{ph}, and the relevant physical parameters of the NEMS structure, that is beam thickness t, length L, and resonator operational frequency ν.

3. Scaling laws relevant to the appropriate phonon transport regimes and their transition boundaries will be analyzed and compared with results of more microscopic analysis and theory.

4. Analyze both surface-assisted and anharmonic coupling of flexural modes with thermalized phonons, focusing especially on treatment of the non-equilibrium phonons in the limit of the high frequency fundamental mode of the resonator.

5. Formulate robust treatment of phonons under non-equilibrium thermodynamic conditions in flexural nanobeams by introducing Boltzmann (or quantum Wigner-Boltzmann) framework for description of phonon transport; conduct analysis of internal thermal phonon flow inside the beam.

6. Consider how influences of the naturally existing beam surface strain and surface roughness can be integrated into the general description of the phonon flow. Evaluate surface effects and their scaling properties in terms of surface-to-volume importance as the resonator geometry approaches the nanolimit.

7. Develop a reliable quantification of the Q factor and noise characteristics in presence of non-diffusive phonon transport.

Relevance to Army:

NEMS have recently attracted great interest in miniaturized device design and actuation for unique potential in military and dual use civil applications. Their impact is pervasive, spanning the broad fields of metrology, engineering, life science, and medicine. In particular, for Department of Army, NEMS resonators have been the focus of great attention for light-weight, robust, on-chip, high-Q resonators and oscillators for frequency control electronics relevant to secure communications. Also, the possibility of obtaining resonators with high operating frequencies into the 1–10 GHz region, with small mass and high-Q suggests NEMS resonators and cantilevers as candidates for actuators and sensors in smart and autonomous systems with unprecedented sensitivities.

Accomplishments:

- Material parameters were successfully identified for the basic high frequency NEMS resonator designs; "operational frequency vs. spatial dimensions" maps have been established for the NEMS resonator from the Euler-Bernoulli equation including the Timoshenko rotational inertia and shear corrections.

- Major intrinsic dissipative mechanisms related to thermoelastic loss and phonon-phonon interactions and their scaling properties have been identified and strategically mapped to provide insightful physical analysis.

- From the developed scaling studies, it is theoretically noted that, in the 1–10 GHz operational frequency regime, the NEMS resonator thermal dynamics routinely goes beyond the limits of the local temperature approximation, not at all due to the often considered time constraint of the high frequency limit (which requires $\nu \approx \tau_{ph}^{-1}$, with $\tau_{ph} \approx 10$ ps at room temperature), but, in contrast, due to sharp spatial inhomogeneity in strain pattern induced by flexure across the thin ($t < l_{ph}$, with $l_{ph} \approx 50$ nm at $T = 300$ K in Si) beam cross section. This spatial consideration leads to rapid ballistic transfer of phonons across the beam and suppression of the dissipation mechanism associated with the entropy production due to inter-branch

phonon-phonon thermal equilibration. The theoretical analysis is formulated and conducted in the Boltzmann framework to capture the proper phonon dynamics.

- Surface properties are heuristically included into the model description opening avenues to meaningful analytical assessment of the surface effects on the dissipation in NEMS and their effects on surface-to-volume scaling as the resonator scales toward the ultimate NEMS limit; as the resonator shrinks, the surface effects become influential in degrading the Q of the lowest modes of the resonator.

Collaborations and Technology Transfer

- The results of this investigation are shared and discussed on the regular basis with Dr. Madan Dubey of ARL and Dr. Arthur Ballato of CECOM.
- We are in contact with the group of Prof. M. Zikry at NCSU for the possibility of advanced multiscale numerical modeling of these systems.

Resulting Journal Publications

A scientific publication describing heat dissipation in nanoscaled flexural resonators is anticipated.

2 Approach, rationale, and accomplishments

Below we describe details of our results and primary approach. The technical approach considered non-equilibrium heat generation and redistribution processes from mechanical strain during high frequency NEMS operation beyond the conventional heat diffusion and local temperature approximation. A semiclassical phonon dynamical picture was introduced to go beyond the conventional models. Scaling laws relevant to the appropriate phonon transport regimes and their transition boundaries were delineated, analyzed, and compared with results of detailed microscopic descriptions. Thus, the research approach involved scaling analysis, coupled with analytical and numerical modeling of phonon flow and heat redistribution in nanoscale resonators.

2.1 Picture of the beam dynamics.

Flexural modes available to the double clamped resonator for large *length to thickness* aspect ratios $L/t > 10$ can be described analytically by the Euler-Bernoulli equation of solid mechanics in the limit of no energy dissipation, and in the continuum approximation [3, 1]. Applying this long-beam approximation of the Euler-Bernoulli theory, one arrives at the equation for the transverse displacement $u(z,t)$ for an undriven beam along the direction of its length, z, as

$$\rho A \frac{\partial^2 u}{\partial t^2} + \frac{\partial^2}{\partial z^2} EI \frac{\partial^2 u}{\partial z^2} = 0.$$

Here ρ is the material density, A is the area of the beam cross-section, E is the Young modulus, I is the cross-sectional area moment of inertia (bending moment of inertia), and EI is known as the *flexural rigidity* of the beam. The boundary conditions specify the beam clamping conditions. In particular, for the rigidly clamped boundary condition, $u = 0$ and $u' \equiv \partial u/\partial z = 0$. Thus, for the resonator, the eigensolution for a homogeneous beam of length L and rectangular cross section $w \times t$ (i. e., $A = wt$, $I = wt^3/12$), clamped at beam ends at $z = 0$ and $z = L$, can be written in phasor form as

$$u_n(z,t) = U_n(z) e^{i\Omega_n t},$$

where

$$U_n(z) = C_{n1}[\cos(k_n z) - \cosh(k_n z)] + C_{n2}[\sin(k_n z) - \sinh(k_n z)],$$

with frequency

$$\Omega_n = \sqrt{\frac{EI}{\rho A}} k_n^2 = \sqrt{\frac{E}{\rho}} t k_n^2. \tag{1}$$

Here k_n is chosen to satisfy the boundary conditions, and is a solution of the transcendental equation

$$\cos(k_n L)\ \cosh(k_n L) = 1;$$

it is found that $k_n L \approx 4.730,\ 7.853,\ 10.996$ for the first three modes. Normalization for the mode amplitudes is conventionally chosen as

$$\int_0^L dz\, U_n^* U_m = L^3 \delta_{nm}.$$

Similar equations can be derived for the cantilever structure, the difference is in the boundary condition at one end, which, unlike double clamped bridge, is left free for the cantilever.

While the Euler-Bernoulli theory works well for the relatively long beams, the importance of the Timoshenko rotational inertia and shear corrections [4] to the beam dynamics progressively increases for smaller L/t ratios. Of course, our consideration here is limited in both approaches to the small flexural vibrations, before nonlinearities start to build up in the resonator behavior.

As a result of our efforts, material parameters were successfully identified for the basic high frequency NEMS resonator designs; "operational frequency vs. spatial dimensions" maps have been established for the NEMS resonator from the Euler-Bernoulli equation including the Timoshenko corrections.

In Fig. 1 we present such a diagram showing frequency of the Si double clamped NEMS resonator in dependence on the beam length and thickness. Two solid lines present results of calculation of the equi-frequency fundamental mode lines in the framework of the Timoshenko theory allowing arbitrary L/t ratio, while dashed curve is a result of the simple Euler-Bernoulli approximation. Since the mode frequency in the Euler-Bernoulli framework is given by Eq. (1), the dashed curve is simply a straight line in the log–log plot. Overall, for both treatments, the fun-

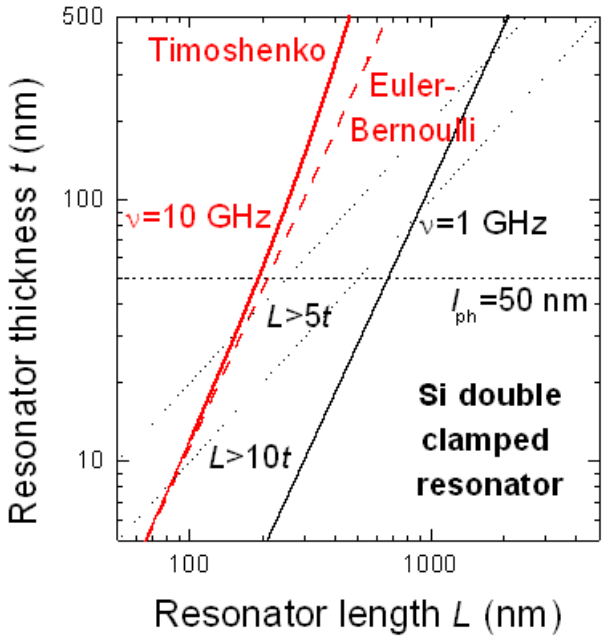

Figure 1: Graphic of NEMS resonator operational frequency $\nu = 1$ GHz and $\nu = 10$ GHz with beam parameters length (L) and thickness (t) from the modified Euler-Bernoulli theory.

damental frequency Ω_1 of the oscillator rises as the resonator size and/or aspect ratio (length to thickness) is reduced, as desired. In this graph we have also shown the phonon mean free path ($l_{ph} \approx 50$ nm in Si at room temperature) on the t axis. The following observations can be made:

- Aspect ratio, L/t, should be large (ideally, greater than 10). Otherwise, deviations from the lowest order Euler-Bernoulli theory increase rapidly (e.g., via Timoshenko corrections); this affects the analytics of NEMS resonator: operational frequency, losses, and limits on magnitude of linear regime.

- 10 GHz resonator with a reasonably large aspect ratio L/t (ideally greater than 10 or at least greater than 5) will inevitably have characteristically small absolute L and t values. In particular, its thickness can routinely be smaller than the phonon mean free path, l_{ph}, establishing regime of ballistic heat transfer in the beam [5]. With progressive scaling of the surface-to-volume ratio, surface effects will also play a significant role.

- Local compression and dilation of the beam material is accompanied by the creation of non-equilibrium phonon distributions and temperature gradients and, consequently, processes of heat redistribution and entropy generation. For beams with substantially large aspect ratios ($L/t > 10$), thermal transport is approximately one-dimensional (and takes place in the plane of the beam cross section); otherwise, the picture of heat redistribution from mechanical strain is complicated and multidimensional.

2.1.1 Structure of the strain field

The structure of the strain field corresponding to a particular flexural mode can be established as follows. For thin beams, the only nonzero components of the strain tensor are defined by the mode deflection amplitude $u(z)$ as

$$u_{zz} = -y\frac{\partial^2 u}{\partial z^2}, \tag{2}$$

$$u_{xx} = u_{yy} = -\sigma u_{zz} \tag{3}$$

where σ is the Poisson ratio. The *trace* of the strain tensor is then

$$\sum_i u_{ii} = -(1-2\sigma)yu''. \tag{4}$$

The strain pattern is visualized in Fig. 2 for the fundamental flexural mode of the double clamped resonator. An important consideration is that, assuming that linear thermal expansion coefficient of the material is not zero, local compression and dilation will be accompanied by the creation of non-equilibrium phonon distributions, temperature gradients and, consequently processes of heat redistribution and entropy generation. Another important observation is that only for beams with large aspect ratios (e. g., L/t greater than 10), thermal transport is approximately one-dimensional.

2.1.2 Mode energy density and total mechanical energy

The linear energy density along the beam is given, in the phasor form, by

$$h_W(z) = \frac{\rho A \Omega^2}{2} \left[U(z)\right]^2 + \frac{EI}{2} \left[U''(z)\right]^2,$$

were the first term is the kinetic energy and the second term is the potential energy of flexural deformation of the beam. In Fig. 3 the diagram, the kinetic energy density, in phasor form, is proportional to the square of the fundamental mode eigenfunction U_1^2 (red line) and the flexural deformation energy is proportional to $(U_1'')^2$ (green line). Both energy distributions are highly uneven along the beam and scale in accordance with L. However, as L is reduced, the *relative* amounts of kinetic and flexural energy along the beam remain unchanged for the Euler-Bernoulli normalized eigenmode U_1; this kinetic-flexural energy partition could vary with L only by considering higher order corrections to the Euler-Bernoulli equation.

Finally, the total energy of the mechanical oscillation is given by

$$W = \int_L dz\, h_W(z). \tag{5}$$

2.2 Intrinsic dissipation mechanisms and their scaling

Numerous mechanisms were previously proposed as possible limitations to the quality factors of micro- and nanoresonators [6, 7, 8, 9]. Losses are of primary importance especially for frequency control devices, as they define noise characteristics by outcome of the *fluctuation-dissipation theorem*. Some mechanisms can be identified as extrinsic to the microresonator and, thus, in principle can be eliminated, while, intrinsic mechanisms, persist due to core material properies of the beam. For example, air damping can be eliminated in the vacuum-operated resonators. Doping impurities, effect of the attachment/support structure, and surface absorption/desorption processes can be accounted for as external.

For intrinsic phonon-mediated dissipation mechanisms, scaling laws can be formulated based

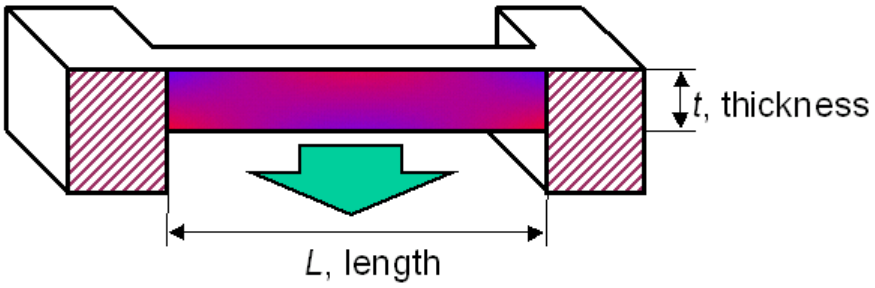

Figure 2: Time-alterating compressive (red) and tensile (blue) strains in the beam are shown at deflection down for the fundamental flexural mode of the double clamped resonator. To recall, we are interested in the limit $L/t \gg 1$, $L \approx$ ultrasubmicron.

on relations between the key spatial and temporal characteristics of phonons, i.e., mean free path l_{ph} and phonon relaxation time τ_{ph}, and the relevant physical parameters of the NEMS structure, that is beam thickness t, length L, and resonator operational frequency ν.

We start with a short review of the relevant phenomena involved in the heat transfer processes on micro- and nanoscale.

2.2.1 Fourier's law

Standard formulation of the equation for the macroscopic heat flow

$$q = -\kappa \nabla T$$

is named Fourier's law and connects heat flow with the temperature gradient. The coefficient of the proportionality is the thermal conductivity κ. The failure of this formulation on the microscopic time and space scales is due to neglectance of the actual physical processes responsible for the heat transfer. Inclusion of these mechanisms leads on the macroscopic level to the appearance of the microscopic build-up time constant τ,

$$q + \tau \frac{\partial q}{\partial t} = -\kappa \nabla T$$

the formulation typically attributed the Cattanco and Vernotte who independently proposed this heuristic generalization. This leads to the so-called hyperbolic heat equation

$$\kappa \nabla^2 T - C_v \frac{\partial T}{\partial t} - \tau C_v \frac{\partial^2 T}{\partial t^2} = -p - \tau \frac{\partial p}{\partial t}.$$

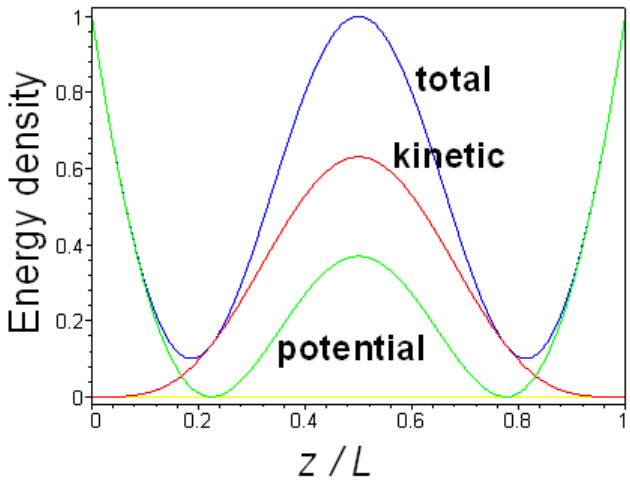

Figure 3: Linear energy density in phasor form for the fundamental flexural mode of the double clamped resonator.

Here C_v is the specific heat, p is the power density. In absence of τ we obtain the classical heat diffusion law. Explicitly,

$$\tau = \frac{3\kappa}{C_v c^2}$$

is the microscopic thermal time. On the macroscopic level, it brings up the phenomenon of the non-diffusive heat transfer by means of the quickly decaying heat waves.

Taking for silicon at room temperature the standard set of parameters $c = 5880$ m/s$= 5.88$ nm/ps, $\kappa = 160$ W/mK, and $C_v = 1.78 \times 10^5$ J/m^{3}K, we obtain for the characteristic *phonon* microscopic time $\tau_{ph} \approx 3{\times}3.5$ ps≈ 10 ps, which corresponds to the phonon mean free path $l_{ph} = c\tau_{ph} \approx 50$ nm.

A different, macroscopic time can be associated in NEMS resonator with the heat diffusion across the beam width as a result of the flexural vibrations. A simple treatment due to Zener [8] reveals

$$\tau_{diff} = \frac{t^2 C_v}{\pi^2 \kappa} = \frac{3}{\pi^2}\left(\frac{t}{c}\right)^2 \frac{1}{\tau_{ph}}.$$

Introducing $\tau_{ballistic} = \sqrt{3}t/c$ — a time neccesary for a typical phonon to ballistically traverse the beam width, we conclude that

$$\tau_{diff} = \frac{1}{\pi^2}\frac{\tau_{ballistic}^2}{\tau_{ph}} = \frac{3}{\pi^2}\frac{t^2}{l_{ph}^2}\tau_{ph}.$$

Thus, quite obviously, for $t \gg l_{ph}$ slow diffusive heat relaxation dominates and the heat transfer is essentially Fourier's transfer.

The standard theory of thermoelastisity relies essentially on the validity of the Fourier heat law [8, 16], thus, either this theory should be upgraded to incorporate non-Fourier's effects in the calculational framework (the path chosen, in particular by Sun et al.[17]; it is worth to mention that estimates suggest that in the interval of parameter values considered in this paper an effect of non-Fourrier heat transfer is minimal), or microscopic relaxation processes should be considered and accoounted for separately in the analysis of intrinsic losses. In case of insulators at elevated temperatures, the specific type of phonon-phonon interactions represent themselves as a so-called Akhiezer effect.

2.2.2 Akhiezer effect

Akhiezer effect is most commonly considered in relation to the losses of ultrasonic waves in dielectric crystals at elevated temperatures and is a result of the phonon-phonon interactions. Due to anharmonicity, strain modulates phonon frequencies (and, strictly speaking, in a different fashion for different phonon modes). As a result, original local equilibrium phonon distribution becomes distorted and requires a microscopic time τ to reestablish phonon equilibrium locally. This irreversible process requires absorption of elastic energy to generate entropy in the phonon sybsystem. A simple qualitative treatment was published by Bömmel and Dransfeld [13]. Essentially, they have split phonon modes in two groups - those, experiencing positive temperature changes and those, experiencing negative or no changes. At the same time, no intragroup deviation from

the equilibrium distribution was assumed. Thus, intergroup temperature relaxation was the main process, giving

$$Q^{-1} = \frac{A}{\Omega} \propto \frac{C_v T \gamma^2}{E} \Omega\tau$$

at sufficiently low frequencies of the acoustic vibrations $\Omega\tau \ll 1$. Here $\gamma =< \gamma_{jk} >$ is the average Grüneisen constant

$$(\Delta c/c)_{jk} = \gamma_{jk}(\Delta\rho/\rho),$$

defined by the material anharmonicity (as given by third-order elestic moduli, or, e. g., related to the temperature expansion coefficient α_T as $\gamma = 3\alpha_T K/C_v$).

It is interesting to see that expressing γ via α_T and K via $E \approx 3K$ in the prefactor for microscopic losses Q^{-1}, and making use of $C_v \approx C_p$, we readily recover the conventional thermoelastic prefactor $\alpha_T^2 TE/C_p$. Of course, a number of approximations led to this coinsidence, in particular, assumption of the high temperature $T > \Theta_D$, which is obviously questionable at room temperature for the silicon with $\Theta_D = 665$ K, assumption of the simple Debye phonon spectrum, and the validity of the application of the Grüneisen constant average.

More advanced microscopic treatment was proposed by Woodruff and Ehrenreich [12], we return to this publication later.

2.2.3 Scaling of losses with resonator dimensions

Applying results of these early developments, we have analyzed major intrinsic dissipative mechanisms related to thermoelastic loss [10] and phonon-phonon interactions [11]. Their scaling properties have been identified and strategically mapped to provide insightful physical analysis. Specifically, from the developed scaling studies, it was theoretically noted that, in the 1–10 GHz operational frequency regime, the NEMS resonator thermal dynamics routinely goes beyond the limits of the local temperature approximation, not at all due to the often considered time constraint of the high frequency limit (which requires $\nu \approx \tau_{ph}^{-1}$, with $\tau_{ph} \approx 10$ ps at room temperature), but, in contrast, due to sharp spatial inhomogeneity in strain pattern induced by flexure across the thin ($t < l_{ph}$, with $l_{ph} \approx 50$ nm at $T = 300$ K in Si, see Fig. 4) beam cross section. This spatial consideration leads, qualitatively, to rapid ballistic transfer of phonons across the beam and suppression of the dissipation mechanism associated with the entropy production due to inter-branch phonon-phonon thermal equilibration. It is further noted that the more consistent theoretical analysis should be formulated and conducted in the Boltzmann framework to capture the proper phonon dynamics.

2.3 Phonons under non-equilibrium thermodynamic conditions in flexural nanobeams

A quantitative description of the processes of heat generation and redistribution in thin flexural beams has been achieved by applying the Boltzmann formalism to capture dynamics of the non-equilibrium phonon distribution resulting from the spatially inhomogeneous mechanical compres-

sion and dilation. The multidimensional integro-differential equation has been derived for the phonon distribution function, encompassing effects of the modulation of the phonon frequencies with applied spacially inhomogeneous strain, phonon ballistic transfer, and scattering processes, leading to thermalization in the phonon ensemble. This allowed a reliable quantification of the resonator quality factor Q in presence of non-diffusive phonon transport.

2.3.1 Phonon Hamiltonian in presence of strain

The phonon Hamiltonian for a particle with wave vector $\mathbf{q}$ (for simplicity of notation, $\mathbf{q}$ includes both the wave vector and the index of the phonon branch) is

$$H = \hbar\omega(\mathbf{q}, \mathbf{r}, t) = \hbar\omega_0(\mathbf{q}) \left[1 + \alpha(\mathbf{q}, \mathbf{r}, t)\right].$$

In the presence of strain, in the lowest order [11]

$$\alpha(\mathbf{q}, \mathbf{r}, t) = -\sum_{ik} \gamma_{ik}(\mathbf{q}) u_{ik}(\mathbf{r}, t),$$

where u_{ik} is the strain tensor and $\gamma_{ik}(\mathbf{q})$ is the *generalized Grüeneisen tensor* [12]. The only non-zero components of the strain tensor in the beam were given in Eqs. (2), (3) above. With that, we can write explicitly

$$\alpha(\mathbf{q}, \mathbf{r}, t) = \left[(1+\sigma)\gamma_{zz}(\mathbf{q}) - \sigma \sum_i \gamma_{ii}(\mathbf{q})\right] y u''(z).$$

Now identifying all diagonal components γ_{ii} of the tensor with *the single Grüneisen constant γ in the theory of the thermal expansion*, we can simplify further, so that

$$\alpha(\mathbf{q}, \mathbf{r}, t) = -\gamma \sum_i u_{ii} = (1 - 2\sigma)\gamma y u''(z). \tag{6}$$

This simplification that γ is scalar and q-independent was historically made in the early development of bulk thermal expansion theory and has served fairly well in simple situations requiring exclusively phonon bulk averages; in the limiting case where the nanoregime is in effect, averaging with respect to $\sum_i \gamma_{ii}$ and γ_{zz} is not so easily justifiable, especially when one needs to accomodate the physically dictated inherent anisotropy into the analysis of the degradation processes. For example, reducing to a single constant, γ, *artificially eradicates* the Akhiezer effect. Therefore, to preserve the physical consequences of the Akhiezer phenomenology, especially at the NEMS spatial and frequency scale, where the effect is particularly important, one should allow for at least two different constants γ_1 and γ_2 to mimic the variation in tensor $\gamma_{ij}(\mathbf{q})$. A simple qualitative treatment of the Akhiezer effect is then possible, as originally provided by Bömmel and Dransfeld [13]. As their starting point, they have split all phonon modes in two distinguished groups — those, experiencing positive temperature changes and those, experiencing negative or no temperature changes.

2.3.2 Boltzmann equation

Our quantitative description of the processes of heat generation and redistribution in thin flexural beams has been achieved by applying the Boltzmann formalism to capture dynamics of the non-equilibrium phonon distribution resulting from the spatially inhomogeneous mechanical compression and dilation. Introducing the instant distribution function $N(\mathbf{q}, \mathbf{r}, t)$ for the population of the phonons in the beam, a thermal equlibrium distribution function

$$N_0(\omega, T) \equiv N_0(\hbar\omega/kT) = \left[\exp(\hbar\omega/kT) - 1\right]^{-1},$$

its derivative N_0' in respect to $x = \hbar\omega/kT$, further splitting N into the "equilibrium" part $N_0(\hbar\omega/kT_0)$, corresponding to the local phonon frequencies ω (defined by the spatially inhomogeneous strain) and the *equlibrium* temperature T_0, and the non-equilibrium part $N_1(\mathbf{q}, \mathbf{r}, t) = N(\mathbf{q}, \mathbf{r}, t) - N_0(\hbar\omega/kT_0)$, we can linearize the original Boltzmann equation for the phonon distribution function

$$\left(\frac{\partial N}{\partial t}\right)_{coll} = \frac{\partial N}{\partial t} + \frac{\partial N}{\partial \mathbf{r}} \cdot \frac{\partial \omega}{\partial \mathbf{q}} - \frac{\partial N}{\partial \mathbf{q}} \cdot \frac{\partial \omega}{\partial \mathbf{r}}$$

to arrive at

$$\left(\frac{\partial N}{\partial t}\right)_{coll} = \frac{\partial N_1}{\partial t} + N_0' \frac{\hbar\omega_0}{kT_0} \frac{\partial \alpha}{\partial t} + \mathbf{v}_0 \cdot \frac{\partial N_1}{\partial \mathbf{r}}. \tag{7}$$

Here the mode velocity $\mathbf{v}_0 = \partial\omega_0/\partial\mathbf{q}$. We would like to note that this particular linearization is different from another commonly performed splitting $N = N_0(\omega_0, T_0) + \tilde{N}_1$, where frequency ω_0 is used in the *true* equilibrium part.

Treating the collision term in the effective relaxation time approximation, we let

$$\left(\frac{\partial N}{\partial t}\right)_{coll} = \frac{N - N_0(\omega, T)}{\tau_{ph}}, \tag{8}$$

where $\tau_{ph}(\mathbf{q})$ is the phonon relaxation time. There are a number of subtle issues associated with this equation. First, it is a heuristic approximation to the realistic microscopic description for the phonon-phonon interactions [14]. Even then, actually two classes of phonon-phonon scattering processes take place, *normal* processes that conserve total momentum of the colliding pair and umklapp process, that do not conserve total momentum. As written in Eq. (8), it is implicitly assumed that the umklapp processes dominate, so as the asymptotic phonon distribution can be characterized by a single parameter — local equlibrium temperature T. Further, this local equlibrium temperature T should not be defined by averaging phonon distribution only at a single spatial point; instead, it should be obtained by averaging over the area of the size of about l_{ph}. Thus, it is clear, that T should approach T_0 as the beam thickness becomes smaller than l_{ph}. Nevertheless, it can be shown that treating T as a single-point quantitity produces virtually identical results for the losses even in the limit of $t < l_{ph}$.

Now we consider a case of substantially different spatial scales $L \gg t$ for the Euler-Bernoulli-Boltzmann resonator, allowing to assume that all thermal transfer is essentially one-dimensional

and takes place along axis y in the plane of the cross section. Seeking oscillatory solutions of N_1 with flexural fundamental frequency Ω, we obtain

$$(1 - i\Omega\tau_{ph})N_1 - v_0\tau_{ph}\cos\theta N_1' = N_0'\frac{\hbar\omega_0}{kT_0}\left(i\Omega\tau_{ph}\alpha(y) - \frac{T_1}{T_0}\right) \tag{9}$$

with the temperature difference $T_1 = T - T_0$ defined by the total energy balance in scattering processes, i. e.,

$$\int d\mathbf{q}\,\hbar\omega\left(\frac{\partial N}{\partial t}\right)_{coll} = 0. \tag{10}$$

Further progress can be made (i) by assuming the Debye model ($\omega = c_0 q$) with the q-independent velocity $v_0 \equiv c_0$ and (ii) by assuming that the relaxation time τ_{ph} is also phonon mode-independent. Expanding then Eq. (10) to the first order in the relaxation approximation, we obtain

$$\frac{1}{4\pi}\int d\theta\,\sin\theta\int dq\,q^2\hbar\omega(q)N_1 = -\frac{T_1}{2\pi}\int dq\,q^2\left[\frac{\hbar\omega_0(q)}{kT_0}\right]^2 kN_0'. \tag{11}$$

The equation for r.h.s. is easily recognizable: recalling that the specific heat of mode q is

$$S(q) = -\left[\frac{\hbar\omega_0(q)}{kT_0}\right]^2 kN_0',$$

and the heat capacity of the phonon subsystem (per unit volume)

$$C = \frac{1}{2\pi}\int dq\,q^2 S(q),$$

we simply get for the r.h.s. of Eq. (11), CT_1.

Now assuming momentarily that the Grüneisen tensor γ is also a q-independent scalar constant as given by Eq. (6), we can multiply Eq. (9) by phonon energy and, integrating it over modulus q, get an equation for

$$f(y,\cos\theta) = \frac{1}{4\pi}\int dq\,q^2\hbar\omega_0 N_1$$

$$(1 - i\Omega\tau_{ph})f - l_{ph}\cos\theta f' = \frac{C}{2}\left[T_1 - i\Omega\tau_{ph}T_0\alpha(y)\right]. \tag{12}$$

Using Eq. (6) expressing $\alpha(y)$ via γ and the flexural mode deflection amlitude $u(z)$, it is also convevient to introduce a function f_γ:

$$f \equiv (1 - 2\sigma)\gamma u''(z) f_\gamma.$$

Here the advantage lies in the explicit factorization of the z dependence, i. e. f_γ is functionally the same along the beam length. The Eq. (12) should be accompanied by the physically meaningful boundary conditions and then solved numerically either directly or as a series expansion. To get a

flavor of the involved mathematics, we mention a particular possible expantion of f

$$f = \sum_n Y_n(y) P_n(\cos\theta) = Y_0 + Y_1 \cos\theta + \dots$$

where $P_n(x)$ are Legendre polynomials. Making use of their properties, one can multiply Eq. (12) for f by various P_m and integrate over angle θ to obtain

$$(1 - i\Omega\tau_{ph})Y_n - l_{ph}\left(\frac{n}{2n-1}Y'_{n-1} + \frac{n+1}{2n+3}Y'_{n+1}\right) = \left(i\Omega\tau_{ph}CT_0\alpha(y) + Y_0\right)\delta_{n0},$$

which should be furhter solved accompanied by appropriate boundary conditions.

2.3.3 Phonon related losses in flexural beams

As it was mentioned above, a conseptually similar problem of sound attenuation in dielectric crystals was considered in [12, 13]. Unlike these publications where an infinite domain with solutions in the form of plane waves was analyzed, here we are forced to operate with solutions on the finite domain in presence of spacial inhomogeneities. The average rate at which the energy is removed from the flexural vibration is equal in the steady state to the rate Z of transfering energy from the phonon system to the heat bath [15]

$$Z = -\sum_{q,j}\left\langle H\left(\frac{\partial N}{\partial t}\right)_{coll}\right\rangle.$$

Using Eq. (7) to express the collisional term via time derivative of N, drift and diffusion terms, and further removing terms that time average to zero, we find

$$Z = \frac{1}{16\pi^3}\int_V d\mathbf{r}\int d\mathbf{q}\,\hbar\omega_0 Re\left\{N_1^*\frac{\partial\alpha}{\partial t}\right\}. \tag{13}$$

With Q^{-1} defined as the fraction of the oscillation energy lost per radian of flexural vibration, total flexural energy W given by Eq. (5), and average rate of energy transfer Z defined by Eq. (13), we arrive at

$$Q^{-1} = \frac{Z}{\Omega W}$$

for the inverse of the resonator quality factor Q.

Invoking previously made approximations of (i) a large beam aspect ratio, (ii) the Debye model, and (iii) constant scalar Grüneisen coefficient, we can perform a number of partial integrations to get, in terms of function f_γ:

$$Z = \Omega\frac{(1-2\sigma)^2\gamma^2 w}{4\pi^2}\int_L dz\;[u''(z)]^2\int_t dy\,y\int d\theta\;\sin\theta\,\mathrm{Im}\left\{f_\gamma\right\}$$

for the particular beam mode $u(z)$. With N_1 (or f) found, phonon-related losses in the beam can

be numerically evaluated.

Again, we stress here that when the assumption of the one dimensional thermal transport (case of a relatively long beam, that is $L \gg t$) is not valid, N_1 cannot be factorized to effectively separate the coordinate z along the beam, then leaving us with a complex system of PDEs to be solved numerically.

2.3.4 Analysis of internal thermal phonon flow inside the beam in the (comparatively simple) limit of large aspect ratio $L/t \gg 1$ ($L \approx$ ultrasubmicron)

Major outcomes of the phenomelogical descriptions can be reproduced, and corresponding characteristic parameters can be established in the framework of the unified formalism:

- Fourier's heat transfer at long times ($t > \tau_{ph}$) and large distances ($l > l_{th}$) [8, 16];
- non-Fourier heat transfer at short times and distances [17]; specifically, since NEMS with GHz frequencies are very small ($t < l_{ph}$), thermoelastic mechanism is dominated by the non-Fourier heat transfer, but, in any case, is of relatively minor importance;

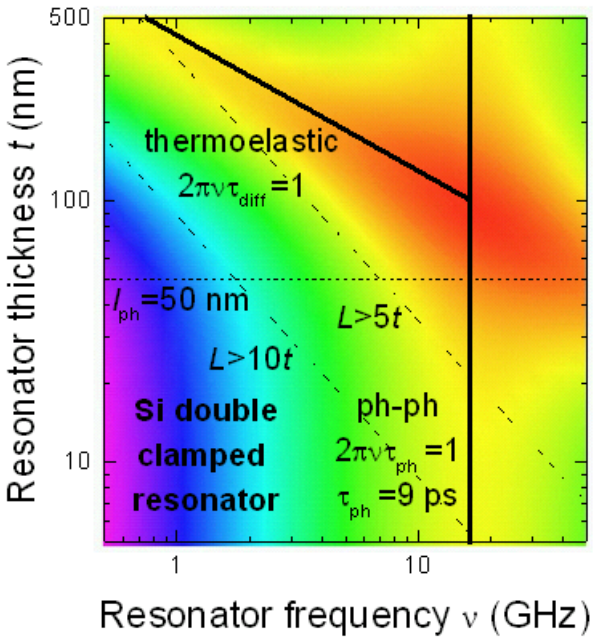

Figure 4: Magnitude of losses. Color code: blue—high Q, low losses, red—low Q, high losses. Here we assume equality of the thermoelastic and microscopic phonon-phonon prefactors, and plot the quality factor for the first flexural mode of the NEMS resonator as a function of the beam length L and thickness t due to both mechanisms together. To stay mostly in the limits of validity of the Euler-Bernoulli theory, one should consider only beams with $L \geq 5t$. While prefactor and τ_{ph} depend only on the material properties, $\Omega_1 \equiv 2\pi\nu_1$ and τ_{diff} are obviously functions of the beam geometry. As one reduces beam dimensions, he can clearly see a crossover in the scaling law around $t =$a few l_{ph}, when, with increasing resonator frequency the thermoelastic mechanism gives in to the phonon-phonon microscopic losses. Quantitatively, for a specific beam aspect ratio $L/t = 10$, a 10 GHz NEMS has substantially higher losses than a 1 GHz resonator.

- distortion by strain of the inter-branch local thermal equilibrium and inter-branch phonon-phonon thermalization—the Akhiezer dissipation mechanism associated with the entropy production due to inter-branch phonon-phonon thermal equilibration [11, 13] actually dominates in small structures.

- In quantitative terms, a 10 GHz silicone NEMS resonator with $L = 10t$ has substantially higher losses than a 1 GHz resonator.

2.4 Surface effects

Rather common outcome of numerical simulatons and experimental observations in MEMS is that the reduction of the resonator size leads to a substantial reduction in the quality factor Q [18, 19]. A feasible explanation for this trend is that microresonator mechanical losses are determined to a great degree by microstructure surfaces and surface-assisted processes. With down-scaling of the resonator, a larger fraction of the beam atoms are found at the surface. Indeed, $a_0 S/V$ grows linearly with reduction of the beam. A word of caution should be given, although: as it was shown above, progressive miniaturazation directly leads to the increase in the frequency of the fundamental mode and, consequently, growth of the losses due to the Akhiezer effect. Coincidentally, the scaling law for this mechanism also follows the S/V dependence.

Experimental work by Mihailovich and MacDonald [18] suggest a presence of losses due to irregularities and damage of the crystal structure in the vicinity of the reactive-ion etched surfaces. Obviously, their relative influence will extend with reduction of the resonator. Damage-healing treatment was suggested to overcome this negative effect, considering that the NEMS structure can withstand them. It was shown that, for example, thermal oxidation can reduce losses due to etched surfaces by a factor of two.

Surface tension and the possible reconstruction on the surface lead to the size-dependence of the effective elastic modulii and material density, the phenomenon observed experimentally [20], as well as in the numerical simulation [19]. Authors of [19] even suggest that they were also able to identify effects of the reconstruction of the material at *corners* of the beam. These effects of surface on the effective material constants directly contribute to the further deviation from the established scaling laws for the resonator frequency, but only indirectly and negligibly to the loss factors. A different mechanism — notable enhancement of the third- and fourth-order anharmonic phonon-phonon interaction in presence of the static strain in the surface layer could leads to the direct dependence of the τ_{ph}^{beam} on the surface-to-volume ratio. For example, one can qualitatively write

$$\frac{1}{\tau_{ph}^{beam}} \approx \frac{1}{\tau_{ph}^{bulk}} + \frac{a_0 S}{V} \frac{1}{\tau_{ph}^{surf}}$$

where, presumbly, $\tau_{ph}^{surf} \ll \tau_{ph}^{bulk}$.

2.4.1 Boundary conditions at beam interfaces for phonon distribution function

We have developed a heuristic approach to incorporate both surface-assisted and anharmonic coupling of flexural modes with thermalized phonons, focusing especially on treatment of the non-equilibrium phonons in the limit of the high frequency fundamental mode of the resonator. As a result, influences of the naturally existing beam surface strain and surface roughness could be integrated into the general description of the phonon flow through a set of heuristic parameters describing scattering and thermalization due to interfaces. For example, one can heuristically force the phonon distribution N to satisfy the physically meaningful boundary condition for the *partial* specular reflection, i. e.,

$$N|_{\pi-\theta} = pN|_{\theta<\pi/2} + (1-p)N_0(\omega, T_b), \tag{14}$$

or, linearized in terms of the N_1

$$N_1|_{\pi-\theta} = pN_1|_{\theta<\pi/2} - (1-p)N_0' \frac{\hbar\omega}{kT_0}\frac{T_{b1}}{T_0}, \tag{15}$$

Here the parameter $0 \leq p \leq 1$ quantifies the part of reflected phonons: p is unity for perfect specular reflection and zero for no specular reflection contribution; we further assume that the complementary part, $(1-p)$, is *instantly thermalized* due to interaction with the interface—this assumption is actually slightly different than the usual assumption of isotropic diffusive scattering [21]. Further, $T_b = T_0 + T_{b1}$ is the local boundary temperature. This approach allows for incorporation of surface effects and estimation of their scaling properties in terms of surface-to-volume importance as the resonator geometry approaches the nanolimit.

It is noted that the influence of "total" thermalization $(1-p)$ at interfaces can be qualitatively interpreted in the following way — assuming dominating ballistic transfer of phonons across the width of the beam, then it follows as a consequence that

$$\frac{1}{\tau_{ph}^{beam}} \approx \frac{1}{\tau_{ph}^{bulk}} + \frac{1-p}{\tau_{ballistic}},$$

which means that the position of the phonon loss peak in the lower part of Fig. 4 shifts away from its original vertical location at approximately $\Omega\tau_{ph}^{bulk} = 1$ as a function of the specularity coefficient p. Therefore, one can expect an influence of p on the intensity of degradation processes and, therefore, Q in the high frequency limit.

From this vignette, one can see an excellent opportunity to explore further the overall importance of surface connected behavior on scaling properties of NEMS structures in a user friendly and quantitative manner.

2.5 Final observations

In summary, we have considered non-equilibrium heat generation and redistribution processes from mechanical strain during high frequency NEMS operation beyond the conventional heat dif-

fusion and local temperature approximation. A semiclassical phonon dynamical picture was introduced to go beyond the conventional models. Scaling laws relevant to the appropriate phonon transport regimes and their transition boundaries were delineated and analyzed; the advanced theoretical analysis was formulated and conducted in the Boltzmann framework to capture the proper phonon dynamics inside flexural beams. Further, surface properties were heuristically included into the model description opening avenues to meaningful analytical assessment of the surface effects on the dissipation in NEMS.

As a result of this study, the intrinsic mechanisms and related analytic principles defining NEMS degradation with scaling have been developed, and have been expressed in a user friendly form for application. It is timely, therefore, to consider a follow on study to pursue the analytic and numerical application of the developed principles so that realistic values of Q can be calculated for actual resonator materials and geometries.

References

[1] A. N. Cleland, *Foundations of Nanomechanics* (Springer-Verlag, Berlin, 2003).

[2] J. A. Pelesko and D. H. Bernstein, *Modeling MEMS and NEMS* (CRC Press, 2002).

[3] L. D. Landau and E. M. Lifshitz, *Theory of Elasticity* (Pergamon Press, Oxford, 1959).

[4] S. P. Timoshenko, J. N. Goodier, *Theory of elasticity* (McGraw-Hill Publishing Co, 1970).

[5] T. S. Tighe, J. M. Worlock, and M. L. Roukes, Appl. Phys. Lett. **70**, 2687 (1997); K. C. Schwab, *et al*., Nature **404**, 974 (2000).

[6] A. S. Novick and B. S. Berry, *Anelasic Relaxation in Crystalline Solids* (Academic Press, New York, 1972).

[7] W. Voigt, *Lehrbuch der Kristallphysik* (Teubner, Leipzig, 1928); A. Ballato, IEEE Trans. on Sonics and Ultrasonics **SU-25**(2), 107 (1978).

[8] C. Zener, Phys. Rev. **52**, 230 (1937); **53**, 90 (1938).

[9] A. N. Cleland and M. L. Roukes, J. Appl. Phys. **92**, 2758 (2002).

[10] R. Lifshitz and M. L. Roukes, Phys. Rev. B **61**, 5600 (2000).

[11] A. Akhiezer, J. Phys. (USSR) **1**, 277 (1939).

[12] T. O. Woodruff and H. Ehrenreich, Phys. Rev. **123**, 1553 (1961).

[13] H. E. Bömmel and K. Dransfeld, Phys. Rev. **117**, 1245 (1960).

[14] P. G. Klemens, In *Lattice Dynamics* IIIB, ed. by W. P. Mason (Academic Press, New York, 1965), p. 201.

[15] E. I. Blount, Phys. Rev. **114**, 418 (1959).

[16] F. L. Guo and G. A. Rogerson, Mech. Research Commun. **30**, 513 (2003).

[17] Y. Sun, D. Fang, and A. K. Soh, Int. J. Solids and Struct. **43**, 3213 (2006).

[18] R. E. Mihailovich and N. C. MacDonald, Sensors and Actuators A **50**, 199 (1995).

[19] R. E. Rudd and J. Q. Broughton, J. Model. and Sim. of Microsys. **1**, 29 (1999); J. Q. Broughton, C. A. Meli, P. Vashishta, and R. K. Kalia, Phys. Rev. B **56**, 611 (1997).

[20] C.-Y. Nam, P. Jaroenapibal, D. Tham, D. E. Luzzi, S. Evoy, and J. Fisher, Nanolett. **6**, 153 (2006).

[21] J. M. Ziman, *Electrons and Phonons: The Theory of Transport Phenomena in Solids* (Oxford University Press, Oxford, 2001).